DOI: 10.26565/2304-6201-2019-44-01

UDC 532.542

Flow modelling in a straight rigid-walled duct with two rectangular axisymmetric narrowings. Part 1. A theory

A. O. Borysyuk
Institute of Hydromechanics of the NAS of Ukraine, 03680, Kyiv 180 MSP, Ukraine
e-mail: aobor@ukr.net

A method for modelling the flow in a rigid-walled duct with two narrowings has been developed. It has the second order of accuracy in the spatial and the first order of accuracy in the temporal coordinates, provides high stability of the solution, and compared to the similar methods requires much less computational time to obtain a result. According to the method, the stream function and the vorticity are introduced initially, and consequently the transition from the governing equations, as well as the initial and boundary conditions to the proper relationships for the introduced variables is performed. The obtained relationships are rewritten in a non-dimensional form. After that a computational domain and a uniform computational mesh are chosen, and the corresponding discretization of the non-dimensional relationships is performed. Finally, the linear algebraic equations obtained as a result of the discretization are solved.

Keywords: *flow, duct, narrowing, stream function, vorticity, pressure.*

Розроблено метод, який дозволяє моделювати течію у прямому плоскому жорсткому каналі з двома прямокутними осесиметричними жорсткими звуженнями. Цей метод має другий порядок точності по просторових і перший порядок точності по часовій координатах, забезпечує високу стійкість розв'язку і потребує значно менше комп'ютерного часу для одержання результату у порівнянні з відповідними методами, які є в науковій літературі. Відповідно до розробленого методу, розв'язування задачі, сформульованої у розділі 2 статті, починається із введення функції течії та завихореності і подальшого переходу від рівнянь Нав'є-Стокса і нерозривності, а також початкових і граничних умов до відповідних співвідношень для введених змінних (підрозділ 3.1 статті). Одержані у такий спосіб співвідношення переписуються у безрозмірній формі (підрозділ 3.2 статті) і дискретизуються у вузлах вибраної просторово-часової сітки інтегрування з малими сталими кроками по часу та координатах (підрозділ 3.3 статті). Після цього розв'язуються лінійні алгебраїчні рівняння для функції течії, завихореності і тиску (підрозділ 3.4 статті), одержані внаслідок проведення зазначеної дискретизації. Щодо останньої, то в ній застосовуються одностороння різниця вперед для дискретизації нестаціонарного члена рівняння переносу завихореності, а також односторонні різниці проти потоку (для дискретизації конвективного члена цього рівняння) та триточкові шаблони (для дискретизації дифузійного члена зазначеного рівняння та рівнянь Пуассона для функції течії і тиску) по осьовій та поперечній координатах. Дискретизація ж компонент швидкості проводиться на основі відповідних центральних різниць. Що стосується зазначених вище лінійних алгебраїчних рівнянь для шуканих величин, то для функції течії і тиску вони розв'язуються за допомогою ітераційного методу послідовної верхньої релаксації. Натомість одержане алгебраїчне співвідношення для завихореності вже є готовою обчислювальною схемою для визначення цієї величини на основі відомих значень відповідних величин, знайдених у попередній момент часу.

Ключові слова: *течія, канал, звуження, функція течії, завихореність, тиск.*

Разработан метод, позволяющий моделировать течение в жестком канале с двумя сужениями. Он имеет второй порядок точности по пространственным и первый порядок точности по временной координатам, обеспечивает высокую устойчивость решения и требует значительно меньше компьютерного времени для получения результата в сравнении с методами подобного типа. Согласно разработанному методу, решение задачи начинается с введения функции течения и завихренности и соответствующего перехода к уравнениям, граничным и начальным условиям для этих переменных. Полученные соотношения переписываются в безразмерном виде и дискретизируются в узлах выбранной равномерной сетки интегрирования. После этого решаются линейные алгебраические уравнения для функции течения, завихренности и давления, полученные вследствие проведения указанной дискретизации.

Ключевые слова: *течение, канал, сужение, функция течения, завихренность, давление.*

1. Introduction

Study of flows in straight channels is an actual problem in many spheres of science and technology. Studying fluid motions in ducts with local narrowings, such as wall deposits, welding joints, stenosis and so on is of a particular interest. That is due to local changes in the flow structure and character, as well as changes in the flow local and integral characteristics and others are caused by such irregularities in the duct geometry. Those changes can have corresponding consequences (sometimes serious) not only in the vicinity of, but far from the irregularities as well (see, for example, [1-13] and the references therein).

An analysis of appropriate publications shows that flows in channels with local narrowings have been studied rather intensively. In those studies, rigid-walled channels and their narrowings are considered, and the simplest narrowing shapes are chosen. As for the basic flow (i.e., the flow upstream of a (first) narrowing), it is laminar, axisymmetric and steady, whereas fluids are assumed to be homogeneous, incompressible and Newtonian. The other types of channels, their narrowings, fluids and the basic flow are not considered in this paper, because they have been studied not so often compared with the ones

mentioned above. Those allow us to investigate the role of the basic parameters of channel, its narrowing and the basic flow within the framework of the appropriate models as well as significantly simplify solutions for the corresponding problems (see, for example, [1-13]).

Among the results obtained, the numerical methods, which have been developed to study flows near channel narrowings, are of a great importance. In particular, a numerical method to solve a problem of flow in an infinite straight hard-walled channel with two rectangular axisymmetric rigid narrowings has been developed in [14]. That method has a second order of accuracy in the temporal and spatial co-ordinates, and allows studying the fluid motion with the velocity and pressure as the variables. However, due to the huge amount of mathematical operations, it requires a lot of computational time to obtain a solution.

In this paper, an alternative method has been developed to solve the same problem with the stream function, vorticity, and pressure as the variables. This method has almost the same order of accuracy and a higher stability of solution, and, due to the use of less powerful mathematical apparatus, requires far less computational time to obtain a result in comparison with the mentioned above.

The paper consists of an introduction (Section 1), three main sections and a list of references. It begins with formulating the problem (Section 2) and presenting the corresponding governing equations, as well as the boundary and initial conditions. The solution method to the formulated problem is described in Section 3. The conclusions of the research are summarized in Section 4 and the list of references is presented.

2. Formulation of the problem

An immovable infinite flat straight rigid-walled duct of width D_0 is considered (Fig.1). This duct has two rigid rectangular axisymmetric narrowings of diameters d_i and lengths l_i $(i=1,2)$, which are situated at the distance l_{12} from one another. In this duct, an incompressible viscous homogeneous Newtonian fluid, of mass density ρ and kinematic viscosity ν, moves. Its flow upstream of the first narrowing (i.e., the basic flow) is steady and laminar, and is characterised by the flow rate q per unit depth of the duct. It is necessary to study the flow near the narrowings, as well as establish the qualitative and quantitative relationships between its characteristics of interest and the parameters of the basic flow, the duct, its narrowings and the distance between them.

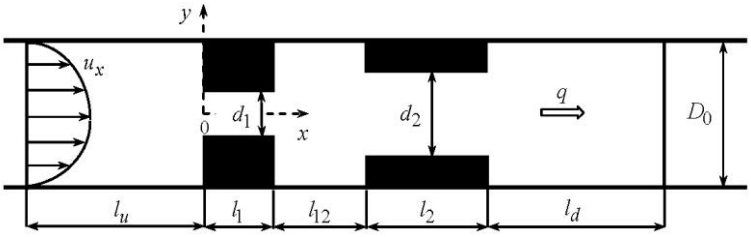

Fig. 1. Geometry of the problem and the corresponding computational domain.

The formulated problem is governed by the two-dimensional Navier-Stokes equations:

$$\frac{\partial u_x}{\partial t}+u_x\frac{\partial u_x}{\partial x}+u_y\frac{\partial u_x}{\partial y}=-\frac{1}{\rho}\frac{\partial p}{\partial x}+\nu\left(\frac{\partial^2 u_x}{\partial x^2}+\frac{\partial^2 u_x}{\partial y^2}\right),$$

$$\frac{\partial u_y}{\partial t}+u_x\frac{\partial u_y}{\partial x}+u_y\frac{\partial u_y}{\partial y}=-\frac{1}{\rho}\frac{\partial p}{\partial y}+\nu\left(\frac{\partial^2 u_y}{\partial x^2}+\frac{\partial^2 u_y}{\partial y^2}\right) \qquad (2.1)$$

and the continuity equation:

$$\frac{\partial u_x}{\partial x}+\frac{\partial u_y}{\partial y}=0. \qquad (2.2)$$

The boundary conditions are zero fluid velocity at the duct wall, S_{ch}, and at the surfaces of both narrowings, S_i, $(i=1,2)$:

$$u_x\big|_{S_{ch},S_i}=0\,,\qquad u_y\big|_{S_{ch},S_i}=0\,. \tag{2.3}$$

Also, due to mass conservation in the duct, the flow rate q must be the same in all cross sections:

$$\frac{\partial q}{\partial x}=0\,,\qquad q=U_a D_0\,. \tag{2.4}$$

In addition, since a laminar basic flow is considered, the parabolic velocity profile is chosen outside the disturbed flow region due to the narrowings (i.e., before the narrowings, where the flow is still undisturbed by them, and far behind them, where the flow is undisturbed again (i.e., where the flow disturbances disappear, and it becomes basic again)):

$$u_x\big|_{x=-l_u,l_1+l_{12}+l_2+l_d}=U_0\left(1-4y^2/D_0^2\right),\qquad u_y\big|_{x=-l_u,l_1+l_{12}+l_2+l_d}=0\,. \tag{2.5}$$

The pressure p is assumed to be constant upstream of the first narrowing:

$$p\big|_{x=-l_u}=\mathrm{const}_u=p_u\,,$$

and far downstream of the second one:

$$p\big|_{x=l_1+l_{12}+l_2+l_d}=\mathrm{const}_d=p_d\,,$$

and the corresponding pressure drop, $\Delta p=p_u-p_d=\mathrm{const}>0$, should ensure the existence of the given laminar regime of the basic flow. Herewith, without loss of generality, the magnitude p_d can be assumed to be zero[1], and the pressure p_u (which now is equal to Δp), like the pressure in the whole channel, needs to be found.

In addition the normal pressure derivative should be zero at the immovable rigid surfaces of the duct and the narrowings:

$$\left.\frac{\partial p}{\partial \mathbf{n}}\right|_{S_{ch}}=0\,,\qquad \left.\frac{\partial p}{\partial \mathbf{n}}\right|_{S_i}=0\,,\qquad i=1,2\,. \tag{2.6}$$

The initial conditions, in absence of fluid motion in the duct, at the instant of time $t=0$ are [14]:

$$u_x\big|_{t=0}=u_y\big|_{t=0}=0\,,\ p\big|_{t=0}=0\,. \tag{2.7}$$

In the relationships (2.1)-(2.7) x and y are the rectangular Cartesian coordinates chosen in such a way that the axis x is directed downstream along the duct axis (see Fig. 1); t the time; u_x and u_y the local fluid velocity components in the directions x and y. U_0 and

$$U_a=\frac{1}{D_0}\int\limits_{-D_0/2}^{D_0/2}u_x\big|_{x=-l_u,l_1+l_{12}+l_2+l_d}\,\mathrm{d}y=\frac{2}{3}U_0$$

are the maximum and averaged (over the channel cross-section) basic flow velocities, respectively. The values of the distances l_u and l_d are given in Subsection 3.3 and the vector $\mathbf{n}$ denotes the outward unit normal to appropriate surface.

3. Solution method

A solution to the problem formulated in the former section consists of the four consecutive steps. The stream function and the vorticity are introduced initially, and the corresponding transition from the variables velocity-pressure to the variables stream function-vorticity-pressure is performed. Then the relationships (which have been obtained on the basis of the transition mentioned above) are rewritten in a non-dimensional form. After that a computational domain and the corresponding space-time computational mesh are chosen, and the corresponding discretization of the non-dimensional relationships is carried out. Finally, the linear algebraic equations obtained after the use of the discretization are solved. Let us consider each of these steps separately.

3.1. Transition to the variables stream function-vorticity-pressure

Introducing the stream function, ψ [15]:

[1] If the value of p_d is fixed, it is always possible to choose the corresponding value of p_u in such a way that the pressure drop Δp (which governs fluid motion in the channel) remains unchangeable.

$$u_x = \frac{\partial \psi}{\partial y}, \quad u_y = -\frac{\partial \psi}{\partial x} \tag{3.1}$$

(which satisfies the equation (2.2)) and the vorticity, ω, (which has only one component in case of two-dimensional flow) [15]:

$$\omega = \frac{\partial u_y}{\partial x} - \frac{\partial u_x}{\partial y} \tag{3.2}$$

allows transiting from the equations (2.1), (2.2) for the velocity and the pressure to the equations for the variables ψ, ω and p. Indeed, taking derivatives of the first and second equations in (2.1) with respect to y and x, respectively, subsequent subtracting the first of the obtained relationships from the second one and taking into account the representation (3.2) gives us the vorticity transfer equation:

$$\frac{\partial \omega}{\partial t} + u_x \frac{\partial \omega}{\partial x} + u_y \frac{\partial \omega}{\partial y} = \nu \nabla^2_{(x,y)} \omega, \tag{3.3}$$

where

$$\nabla^2_{(x,y)} = \frac{\partial^2}{\partial x^2} + \frac{\partial^2}{\partial y^2}$$

is the Laplace operator in the coordinates x, y.

Substituting representation (3.1) into relationship (3.2) yields Poisson's equation for the stream function:

$$\nabla^2_{(x,y)} \psi = -\omega, \tag{3.4}$$

which directly relates the functions ψ and ω with one another.

Afterwards, differentiating the first equation in the system (2.1) with respect to x and the second one in (2.1) with respect to y, adding the obtained relationships to one another and taking into account the continuity equation (2.2) results in Poisson's equation for the pressure:

$$\nabla^2_{(x,y)} p = -\rho \left[\left(\frac{\partial u_x}{\partial x} \right)^2 + 2 \frac{\partial u_x}{\partial y} \frac{\partial u_y}{\partial x} + \left(\frac{\partial u_y}{\partial y} \right)^2 \right]. \tag{3.5}$$

As for the boundary and initial conditions for the variables ψ, ω and p, they can be obtained from the conditions (2.3)-(2.7) with the use of appropriate mathematical operations. In fact, the relationships (2.5) together with (3.1), (3.2) allow us to write conditions for the stream function and the vorticity in the inlet $x = -l_u$ and the outlet $x = l_1 + l_{12} + l_2 + l_d$ sections of the disturbed flow region due to the narrowings:

$$\psi\big|_{x=-l_u, l_1+l_{12}+l_2+l_d} = U_0 y \left(1 - \frac{4y^2}{3D_0^2} \right), \qquad \omega\big|_{x=-l_u, l_1+l_{12}+l_2+l_d} = \frac{8U_0 y}{D_0^2}. \tag{3.6}$$

From a zero normal component of the fluid velocity on the duct and the walls of narrowings (on the basis of (3.1)) the constancy of the function ψ follows:

$$\psi\big|_{S_{ch}^+, S_i^+} = \text{const}_+, \qquad \psi\big|_{S_{ch}^-, S_i^-} = \text{const}_-, \qquad i = 1,2$$

(here S_{ch}^+ and S_i^+ are the upper walls of the channel and the i-th narrowing, respectively, and S_{ch}^- and S_i^- their lower walls). From here, on the basis of the first relationship in (3.6), we obtain the following conditions

$$\psi\big|_{S_{ch}^+, S_i^+} = \frac{1}{3} U_0 D_0, \qquad \psi\big|_{S_{ch}^-, S_i^-} = -\frac{1}{3} U_0 D_0, \qquad i = 1,2. \tag{3.7}$$

The absence of the tangential component of the fluid velocity at the surfaces S_{ch} and S_i yields zero values of the first-order normal derivatives and the second-order mixed derivative of the function ψ:

$$\left.\frac{\partial \psi}{\partial y}\right|_{S_{ch}, S_i^h} = 0, \ \left.\frac{\partial \psi}{\partial x}\right|_{S_i^v} = 0, \qquad \left.\frac{\partial^2 \psi}{\partial x \partial y}\right|_{S_{ch}, S_i} = 0, \qquad i = 1,2 \tag{3.8}$$

(in the conditions (3.8), S_i^h and S_i^{v} denote the horizontal and vertical parts of the surface S_i, respectively).

The relationships (3.8) together with the equation (3.4) allow us to write the following conditions for the vorticity at the channel and the walls of narrowings:

$$\omega\big|_{S_{ch},S_i^h} = -\frac{\partial^2\psi}{\partial y^2}\bigg|_{S_{ch},S_i^h}, \qquad \omega\big|_{S_i^{\mathrm{v}}} = -\frac{\partial^2\psi}{\partial x^2}\bigg|_{S_i^{\mathrm{v}}}, \qquad i=1,2. \tag{3.9}$$

Regarding the boundary conditions for the pressure, we have (apart from conditions (2.6)) the following two conditions:

$$\frac{\partial p}{\partial x}\bigg|_{S_i^{\mathrm{v}}} = \rho\left[\nu\nabla^2_{(x,y)}u_x - \frac{\partial u_x}{\partial t}\right]_{S_i^{\mathrm{v}}}, \qquad \frac{\partial p}{\partial y}\bigg|_{S_{ch},S_i^h} = \rho\left[\nu\nabla^2_{(x,y)}u_y - \frac{\partial u_y}{\partial t}\right]_{S_{ch},S_i^h}, \ i=1,2. \tag{3.10}$$

The relationships (3.10) are obtained from the equations (2.1) after the conditions (2.3) were used.

As for the initial conditions for ψ, ω and p, they are equal to zero at the instant of time $t=0$ (see (2.7)-(3.2)):

$$\psi\big|_{t=0} = 0, \qquad \omega\big|_{t=0} = 0, \qquad p\big|_{t=0} = 0. \tag{3.11}$$

3.2. Non-dimensional relationships

Making computations, it is convenient to deal with non-dimensional analogues of the relationships presented in the previous subsection. Such analogues can be obtained after introducing appropriate scaling coefficients. In this study, the following magnitudes are chosen as the coefficients: the channel width D_0 as the length scale; the cross-sectionally averaged basic flow velocity, $U_a = q/D_0$, as the velocity scale; the ratio D_0/U_a and the double mean dynamic pressure of the basic flow, ρU_a^2, as the time and pressure scales, respectively; the product $U_a D_0$ serves as the scale for both the stream function and the flow rate; and the ratio U_a/D_0 as the scale for the vorticity.

For these coefficients, the non-dimensional analogues of the representations (3.1), (3.2) and the equations (3.3)-(3.5) have the following forms, respectively

$$U_x = \frac{\partial\Psi}{\partial Y}, \qquad U_y = -\frac{\partial\Psi}{\partial X}, \qquad \Omega = \frac{\partial U_y}{\partial X} - \frac{\partial U_x}{\partial Y}, \tag{3.12}$$

$$\frac{\partial\Omega}{\partial T} + U_x\frac{\partial\Omega}{\partial X} + U_y\frac{\partial\Omega}{\partial Y} = \frac{1}{\mathrm{Re}}\nabla^2_{(X,Y)}\Omega, \tag{3.13}$$

$$\nabla^2_{(X,Y)}\Psi = -\Omega, \tag{3.14}$$

$$\nabla^2_{(X,Y)}P = -\left(\frac{\partial U_x}{\partial X}\right)^2 - 2\frac{\partial U_x}{\partial Y}\frac{\partial U_y}{\partial X} - \left(\frac{\partial U_y}{\partial Y}\right)^2. \tag{3.15}$$

The dimensionless analogues of boundary conditions (2.4), (2.6), (3.6)-(3.10) are written as

$$\frac{\partial Q}{\partial X} = 0, \qquad Q = 1, \quad \frac{\partial P}{\partial \mathbf{n}}\bigg|_{S_{ch},S_i} = 0, \quad \Psi\big|_{X=-L_u,L_1+L_{12}+L_2+L_d} = \frac{3}{2}Y\left(1-\frac{4}{3}Y^2\right),$$

$$\Omega\big|_{X=-L_u,L_1+L_{12}+L_2+L_d} = 12Y, \quad \Psi\big|_{S_{ch}^+,S_i^+} = \frac{1}{2}, \quad \Psi\big|_{S_{ch}^-,S_i^-} = -\frac{1}{2},$$

$$\frac{\partial\Psi}{\partial Y}\bigg|_{S_{ch},S_i^h} = 0, \quad \frac{\partial\Psi}{\partial X}\bigg|_{S_i^{\mathrm{v}}} = 0, \qquad \frac{\partial^2\Psi}{\partial X\,\partial Y}\bigg|_{S_{ch},S_i} = 0,$$

$$\Omega\big|_{S_{ch},S_i^h} = -\frac{\partial^2\Psi}{\partial Y^2}\bigg|_{S_{ch},S_i^h}, \qquad \Omega\big|_{S_i^{\mathrm{v}}} = -\frac{\partial^2\Psi}{\partial X^2}\bigg|_{S_i^{\mathrm{v}}}, \qquad i=1,2, \tag{3.16}$$

$$\frac{\partial P}{\partial X}\bigg|_{S_i^{\mathrm{v}}} = \left[\frac{1}{\mathrm{Re}}\nabla^2_{(X,Y)}U_x - \frac{\partial U_x}{\partial T}\right]_{S_i^{\mathrm{v}}}, \qquad \frac{\partial P}{\partial Y}\bigg|_{S_{ch},S_i^h} = \left[\frac{1}{\mathrm{Re}}\nabla^2_{(X,Y)}U_y - \frac{\partial U_y}{\partial T}\right]_{S_{ch},S_i^h}.$$

The initial conditions (3.11) for the dimensionless variables Ψ, Ω and P are rewritten in the following way

$$\Psi\big|_{T=0} = 0, \qquad \Omega\big|_{T=0} = 0, \qquad P\big|_{T=0} = 0. \tag{3.17}$$

In the relationships (3.12)-(3.17) $X = x / D_0$ and $Y = y / D_0$ are the dimensionless coordinates x and y; $T = tU_a / D_0$ the dimensionless time; $U_x = u_x / U_a$ and $U_y = u_y / U_a$ the dimensionless fluid velocity components in the directions x and y; $\Psi = \psi / (D_0 U_a)$ and $\Omega = \omega D_0 / U_a$ the dimensionless stream function and vorticity, respectively; $P = p / (\rho U_a^2)$ the non-dimensional pressure; $\mathrm{Re} = U_a D_0 / \nu$ the Reynolds number of the cross-sectionally averaged basic flow; $Q = q / (U_a D_0)$ the non-dimensional flow rate in the channel per its unit depth; $D_i = d_i / D_0$ and $L_i = l_i / D_0$ the dimensionless diameters d_i and lengths l_i ($i = 1, 2$), respectively; $L_u = l_u / D_0$ and $L_d = l_d / D_0$ the dimensionless distances l_u and l_d;

$$\nabla^2_{(X,Y)} = \frac{\partial^2}{\partial X^2} + \frac{\partial^2}{\partial Y^2}$$

the Laplace operator in the coordinates X, Y. It is also taken into account that $U_a = 2U_0 / 3$ (see after the conditions (2.7)).

3.3. Computational domain, computational mesh and discrete relationships

The domain, in which a solution to the formulated problem should be found, is shown in Fig. 1. Its left boundary $X = -L_u$ is taken upstream of the first narrowing, where the flow is undisturbed by it, and the right boundary, $X = L_1 + L_{12} + L_2 + L_d$, behind the second narrowing, where the flow is already undisturbed (i.e., where the flow disturbances disappear, and it redevelops into the basic one). Herewith, for the basic flow velocity the values of the distances L_u and L_d considered in this study are assumed to vary in the following ranges [14]

$$L_u \le 0.5, \qquad L_d \le 12.$$

In the indicated domain, a uniform rectangular computational mesh having small spacings (steps) Δ_X and Δ_Y in the directions X and Y, respectively, is introduced (Fig. 2):

$$X_n = X_{n-1} + \Delta_X, \ \Delta_X = \mathrm{const}_X << 1; \ Y_m = Y_{m-1} + \Delta_Y, \ \Delta_Y = \mathrm{const}_Y << 1. \tag{3.18}$$

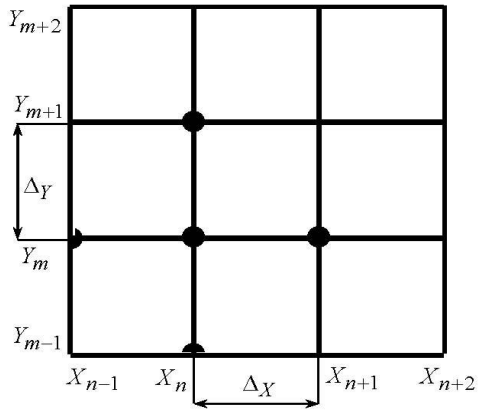

Fig. 2. Computational mesh.

The integration time is divided into small intervals of the constant duration Δ_T:

$$T_k = T_{k-1} + \Delta_T = k\Delta_T, \ \Delta_T = \mathrm{const}_T << 1, \ T_0 = 0. \tag{3.19}$$

Afterwards a discretization of the relationships (presented in the previous subsection) at the nodes X_n, Y_m, T_k of the computational grid (3.18), (3.19) is carried out. In doing so the values of an arbitrary magnitude f at the space-time point X_n, Y_m, T_k are denoted by $f^k_{n,m}$:

$$f_{n,m}^{k} = f(X,Y,T)\big|_{X=X_n,Y=Y_m,T=T_k}.$$

Discrete analogues of the dimensionless governing equations

Discrete analogues of the representations (3.12) for the velocity components are obtained after applying the appropriate central differences to them [15]:

$$\left(U_x\right)_{n,m}^{k} = \frac{\Psi_{n,m+1}^{k} - \Psi_{n,m-1}^{k}}{2\Delta_Y}, \quad \left(U_y\right)_{n,m}^{k} = -\frac{\Psi_{n+1,m}^{k} - \Psi_{n-1,m}^{k}}{2\Delta_X}. \tag{3.20}$$

The relationships (3.20) have the second order of accuracy (a discrete analogue of the representation (3.12) for the vorticity is not presented because it is not used in the paper).

In order to discretize the equation (3.13), we use the two-point temporal onward differencing scheme, as well as the two-point backward differences and the three-point approximations (or the two-dimensional five-point differencing scheme; see Fig. 2) in the corresponding coordinates [15]. Specifically, the application of the two-point temporal onward difference to the non-steady term in (3.13) yields its discrete counterpart of the first order of accuracy:

$$\left(\frac{\partial\Omega}{\partial T}\right)_{n,m}^{k} = \frac{\Omega_{n,m}^{k+1} - \Omega_{n,m}^{k}}{\Delta_T}. \tag{3.21}$$

The convective term of the equation (3.13) is discretized by the two-point backward difference schemes in the coordinates X and Y having the second order of accuracy:

$$\left(U_x\frac{\partial\Omega}{\partial X}\right)_{n,m}^{k} = \begin{cases} \left(U_x\right)_{n,m}^{k}\dfrac{\Omega_{n,m}^{k} - \Omega_{n-1,m}^{k}}{\Delta_X}; \left(U_x\right)_{n,m}^{k} \geq 0, \\ \left(U_x\right)_{n,m}^{k}\dfrac{\Omega_{n+1,m}^{k} - \Omega_{n,m}^{k}}{\Delta_X}; \left(U_x\right)_{n,m}^{k} < 0, \end{cases}$$

$$\left(U_y\frac{\partial\Omega}{\partial Y}\right)_{n,m}^{k} = \begin{cases} \left(U_y\right)_{n,m}^{k}\dfrac{\Omega_{n,m}^{k} - \Omega_{n,m-1}^{k}}{\Delta_Y}; \left(U_y\right)_{n,m}^{k} \geq 0, \\ \left(U_y\right)_{n,m}^{k}\dfrac{\Omega_{n,m+1}^{k} - \Omega_{n,m}^{k}}{\Delta_Y}; \left(U_y\right)_{n,m}^{k} < 0. \end{cases} \tag{3.22}$$

A for the diffusive term in (3.13), its discrete analogue of the second order of accuracy is obtained on the basis of the noted five-point scheme:

$$\left(\frac{\partial^2\Omega}{\partial X^2}\right)_{n,m}^{k} = \frac{\Omega_{n+1,m}^{k} - 2\Omega_{n,m}^{k} + \Omega_{n-1,m}^{k}}{\Delta_X^2}, \qquad \left(\frac{\partial^2\Omega}{\partial Y^2}\right)_{n,m}^{k} = \frac{\Omega_{n,m+1}^{k} - 2\Omega_{n,m}^{k} + \Omega_{n,m-1}^{k}}{\Delta_Y^2}. \tag{3.23}$$

The availability of the relationships (3.21)-(3.23), as well as the use of the expressions (3.20) in (3.22) allow us to write a discrete counterpart of the equation (3.13):

$$\Omega_{n,m}^{k+1} = C_{n,m}^{k}\Omega_{n,m}^{k} + C_{n-1,m}^{k}\Omega_{n-1,m}^{k} + C_{n+1,m}^{k}\Omega_{n+1,m}^{k} + C_{n,m-1}^{k}\Omega_{n,m-1}^{k} + C_{n,m+1}^{k}\Omega_{n,m+1}^{k}, \tag{3.24}$$

in which the coefficients have the following forms:

$$C_{n,m}^{k} = \begin{cases} 1 - \alpha_{XY}\left(\left(\Delta\Psi\right)_{n,m,Y}^{k} - \left(\Delta\Psi\right)_{n,m,X}^{k}\right) - 2\alpha_X - 2\alpha_Y; \left(U_x\right)_{n,m}^{k} \geq 0, \left(U_y\right)_{n,m}^{k} \geq 0; \\ 1 - \alpha_{XY}\left(\left(\Delta\Psi\right)_{n,m,Y}^{k} + \left(\Delta\Psi\right)_{n,m,X}^{k}\right) - 2\alpha_X - 2\alpha_Y; \left(U_x\right)_{n,m}^{k} \geq 0, \left(U_y\right)_{n,m}^{k} < 0; \\ 1 + \alpha_{XY}\left(\left(\Delta\Psi\right)_{n,m,Y}^{k} + \left(\Delta\Psi\right)_{n,m,X}^{k}\right) - 2\alpha_X - 2\alpha_Y; \left(U_x\right)_{n,m}^{k} < 0, \left(U_y\right)_{n,m}^{k} \geq 0; \\ 1 + \alpha_{XY}\left(\left(\Delta\Psi\right)_{n,m,Y}^{k} - \left(\Delta\Psi\right)_{n,m,X}^{k}\right) - 2\alpha_X - 2\alpha_Y; \left(U_x\right)_{n,m}^{k} < 0, \left(U_y\right)_{n,m}^{k} < 0; \end{cases}$$

$$C^k_{n-1,m}=\begin{cases}\alpha_{XY}(\Delta\Psi)^k_{n,m,Y}+\alpha_X;(U_x)^k_{n,m}\ge 0,\left(U_y\right)^k_{n,m}\ge 0;\\ \alpha_{XY}(\Delta\Psi)^k_{n,m,Y}+\alpha_X;(U_x)^k_{n,m}\ge 0,\left(U_y\right)^k_{n,m}<0;\\ \alpha_X;(U_x)^k_{n,m}<0,\left(U_y\right)^k_{n,m}\ge 0;\\ \alpha_X;(U_x)^k_{n,m}<0,\left(U_y\right)^k_{n,m}<0;\end{cases}$$

$$C^k_{n+1,m}=\begin{cases}\alpha_X;(U_x)^k_{n,m}\ge 0,\left(U_y\right)^k_{n,m}\ge 0;\\ \alpha_X;(U_x)^k_{n,m}\ge 0,\left(U_y\right)^k_{n,m}<0;\\ -\alpha_{XY}(\Delta\Psi)^k_{n,m,Y}+\alpha_X;(U_x)^k_{n,m}<0,\left(U_y\right)^k_{n,m}\ge 0;\\ -\alpha_{XY}(\Delta\Psi)^k_{n,m,Y}+\alpha_X;(U_x)^k_{n,m}<0,\left(U_y\right)^k_{n,m}<0;\end{cases}$$

$$C^k_{n,m-1}=\begin{cases}-\alpha_{XY}(\Delta\Psi)^k_{n,m,X}+\alpha_Y;(U_x)^k_{n,m}\ge 0,\left(U_y\right)^k_{n,m}\ge 0;\\ \alpha_Y;(U_x)^k_{n,m}\ge 0,\left(U_y\right)^k_{n,m}<0;\\ -\alpha_{XY}(\Delta\Psi)^k_{n,m,X}+\alpha_Y;(U_x)^k_{n,m}<0,\left(U_y\right)^k_{n,m}\ge 0;\\ \alpha_Y;(U_x)^k_{n,m}<0,\left(U_y\right)^k_{n,m}<0;\end{cases}$$

$$C^k_{n,m+1}=\begin{cases}\alpha_Y;(U_x)^k_{n,m}\ge 0,\left(U_y\right)^k_{n,m}\ge 0;\\ \alpha_{XY}(\Delta\Psi)^k_{n,m,X}+\alpha_Y;(U_x)^k_{n,m}\ge 0,\left(U_y\right)^k_{n,m}<0;\\ \alpha_Y;(U_x)^k_{n,m}<0,\left(U_y\right)^k_{n,m}\ge 0;\\ \alpha_{XY}(\Delta\Psi)^k_{n,m,X}+\alpha_Y;(U_x)^k_{n,m}<0,\left(U_y\right)^k_{n,m}<0;\end{cases}$$

Here the magnitudes α_X, α_Y, α_{XY} are the appropriate ratios of the steps of the space-time computational grid (3.18), (3.19):

$$\alpha_X=\frac{1}{\mathrm{Re}}\frac{\Delta_T}{\Delta_X^2},\ \alpha_Y=\frac{1}{\mathrm{Re}}\frac{\Delta_T}{\Delta_Y^2},\quad \alpha_{XY}=\frac{\Delta_T}{2\Delta_X\Delta_Y},$$

and $(\Delta\Psi)^k_{n,m,X}$ and $(\Delta\Psi)^k_{n,m,Y}$ the increases of the function Ψ in the X and Y directions of the grid, respectively:

$$(\Delta\Psi)^k_{n,m,X}=\Psi^k_{n+1,m}-\Psi^k_{n-1,m},\qquad (\Delta\Psi)^k_{n,m,Y}=\Psi^k_{n,m+1}-\Psi^k_{n,m-1}.$$

As for the discrete analogues of Poisson's equations (3.14) (for the stream function) and (3.15) (for the pressure), they look similar:

$$\frac{\Psi^k_{n+1,m}-2\Psi^k_{n,m}+\Psi^k_{n-1,m}}{\Delta_X^2}+\frac{\Psi^k_{n,m+1}-2\Psi^k_{n,m}+\Psi^k_{n,m-1}}{\Delta_Y^2}=-\Omega^k_{n,m},\tag{3.25}$$

$$\frac{P^k_{n+1,m}-2P^k_{n,m}+P^k_{n-1,m}}{\Delta_X^2}+\frac{P^k_{n,m+1}-2P^k_{n,m}+P^k_{n,m-1}}{\Delta_Y^2}=-\left[\left(\frac{\partial U_x}{\partial X}\right)^2+2\frac{\partial U_x}{\partial Y}\frac{\partial U_y}{\partial X}+\left(\frac{\partial U_y}{\partial Y}\right)^2\right]^k_{n,m}.\tag{3.26}$$

The relationships (3.25) and (3.26) have the second order of accuracy and are obtained after application of the two-dimensional five-point differencing scheme to the equations (3.14), (3.15).

The discrete analogues of the dimensionless boundary conditions and their application to the equations (3.20), (3.24)-(3.26)

The discrete analogues of the dimensionless boundary conditions for the stream function and the vorticity from the relationships (3.16) are written as

$$\Psi^k_{n,m}\Big|_{X=-L_u,L_1+L_{12}+L_2+L_d}=\frac{3}{2}Y\left(1-\frac{4}{3}Y^2\right),\quad \Psi^k_{n,m}\Big|_{S^+_{ch},S^+_i}=\frac{1}{2},\quad \Psi^k_{n,m}\Big|_{S^-_{ch},S^-_i}=-\frac{1}{2},$$

$$\left(\Psi^k_{n,m+1}-\Psi^k_{n,m-1}\right)_{S_{ch},S^h_i}=0,\quad \left(\Psi^k_{n+1,m}-\Psi^k_{n-1,m}\right)_{S^{\mathrm{v}}_i}=0,$$

$$\Omega^k_{n,m}\Big|_{X=-L_u,L_1+L_{12}+L_2+L_d}=12Y,\quad \Omega^k_{n,m}\Big|_{S_{ch},S^h_i}=-\left.\frac{\Psi^k_{n,m+1}-2\Psi^k_{n,m}+\Psi^k_{n,m-1}}{\Delta^2_Y}\right|_{S_{ch},S^h_i},$$

$$\Omega\big|_{S^{\mathrm{v}}_i}=-\left.\frac{\Psi^k_{n+1,m}-2\Psi^k_{n,m}+\Psi^k_{n-1,m}}{\Delta^2_X}\right|_{S^{\mathrm{v}}_i},\quad i=1,2.$$

Regarding the pressure P, the discrete counterparts of the corresponding boundary conditions from (3.16) have the following forms:

$$\left(\frac{\partial P}{\partial \mathbf{n}}\right)^k_{n,m}\Bigg|_{S_{ch},S_i}=0,\qquad i=1,2,$$

$$\left(\frac{\partial P}{\partial X}\right)^k_{n,m}\Bigg|_{S^{\mathrm{v}}_i}=\left[\frac{1}{\mathrm{Re}}\left(\frac{(U_x)^k_{n+1,m}-2(U_x)^k_{n,m}+(U_x)^k_{n-1,m}}{\Delta^2_X}+\right.\right.$$

$$\left.\left.+\frac{(U_x)^k_{n,m+1}-2(U_x)^k_{n,m}+(U_x)^k_{n,m-1}}{\Delta^2_Y}\right)-\frac{(U_x)^{k+1}_{n,m}-(U_x)^k_{n,m}}{\Delta_T}\right]_{S^{\mathrm{v}}_i},$$

$$\left(\frac{\partial P}{\partial Y}\right)^k_{n,m}\Bigg|_{S_{ch},S^h_i}=\left[\frac{1}{\mathrm{Re}}\left(\frac{(U_y)^k_{n+1,m}-2(U_y)^k_{n,m}+(U_y)^k_{n-1,m}}{\Delta^2_X}+\right.\right.$$

$$\left.\left.+\frac{(U_y)^k_{n,m+1}-2(U_y)^k_{n,m}+(U_y)^k_{n,m-1}}{\Delta^2_Y}\right)-\frac{(U_y)^{k+1}_{n,m}-(U_y)^k_{n,m}}{\Delta_T}\right]_{S_{ch},S^h_i}$$

(the representation (3.20) should be used for the velocity components).

These relationships allow us to find the values of all terms of the equations (3.20), (3.24)-(3.26) on the boundary of the chosen computational domain (see the very beginning of Subsection 3.3).

The discrete analogues of the dimensionless initial conditions and their application to the equations (3.20), (3.24)-(3.26)

The discrete analogues of the dimensionless initial conditions (3.17) are as follows:

$$\Psi^k_{n,m}\Big|_{k=0}=0,\quad \Omega^k_{n,m}\Big|_{k=0}=0,\qquad P^k_{n,m}\Big|_{k=0}=0.$$

They allow computing the values of all terms of the equations (3.20), (3.24)-(3.26) at the initial instant of time in the computational domain.

3.4. A solution of the equations (3.20), (3.24)-(3.26)

The analysis of the equations (3.24), (3.25) shows that

– at first sight, due to nonlinearity of the right part in (3.24) (whose terms depend of the products $\Psi\Omega$ at the appropriate points of the space-time grid (3.18), (3.19)), this equation is nonlinear;
– they are coupled.

However, more detailed study of the equation (3.24) indicates that all terms in its right part are the known magnitudes (because they are computed at the previous time stage, $T = T_k$, and at the initial instant of time they are established (see above)). Therefore, the relationship (3.24) is a computational scheme (rather than an equation) to determine the vorticity values, $\Omega_{n,m}^{k+1}$, on the basis of its known right part. Accordingly, the system (3.24), (3.25) is not a system of coupled algebraic equations.

The availability of the vorticity values at all the nodes of the integration mesh (3.18), (3.19) (which are obtained on the basis of the scheme (3.24)) allows proceeding to solving the system of linear algebraic equations (i.e., SLAE) (3.25) with a known right part.

In scientific literature, direct and iteration methods are applied to solve SLAE. The former are used in case of SLAE of small dimensions, and present good results. However, when systems of equations are of big dimensions and, in addition, their matrices are rarefied, direct methods require a lot of both time and computational memory. Therefore, their application is unsuitable. Iteration methods need much less computational memory and time to solve SLAE of big dimensions, keep their matrices rarefied (if such a property is present), and give satisfactory results [15].

Taking that into account, as well as the dimension and the rarefaction degree of the matrix of system (3.25), the successive over-relaxation iteration method is chosen [15]. This method has a second order of accuracy, and its computational scheme for SLAE (3.25) has the following form

$$\Psi_{n,m}^{k+1} = (1-\gamma)\Psi_{n,m}^{k} + \frac{\gamma}{2(1+\beta^2)}\left(\Psi_{n+1,m}^{k} + \Psi_{n-1,m}^{k} + \beta^2\Psi_{n,m+1}^{k} + \beta^2\Psi_{n,m-1}^{k} + \Delta_X^2\Omega_{n,m}^{k}\right) \qquad (4.1)$$

(here γ is the relaxation parameter varying in the ranges $1 < \gamma \le 2$, and $\beta = \Delta_X / \Delta_Y$ the ratio of the steps of the grid (3.18)). It could be seen that all terms on the right-hand side of the scheme (4.1) are known values. Therefore, the magnitudes $\Psi_{n,m}^{k+1}$ are found by performing the operations indicated on the right side of (4.1).

The found values of the function Ψ let us determine (on the basis of (3.20)) the corresponding values of the velocity components U_x and U_y, and substitute these values into the right part of the system (3.26). Afterwards the successive over-relaxation method is applied to solve SLAE (3.26):

$$P_{n,m}^{k+1} = (1-\gamma)P_{n,m}^{k} + \frac{\gamma}{2(1+\beta^2)}\left(P_{n+1,m}^{k} + P_{n-1,m}^{k} + \beta^2 P_{n,m+1}^{k} + \beta^2 P_{n,m-1}^{k} + \Delta_X^2 S_{n,m}^{k}\right), \qquad (4.2)$$

$$S_{n,m}^{k} = \left[\left(\frac{\partial U_x}{\partial X}\right)^2 + 2\frac{\partial U_x}{\partial Y}\frac{\partial U_y}{\partial X} + \left(\frac{\partial U_y}{\partial Y}\right)^2\right]_{n,m}^{k}.$$

As in the computational schemes (3.24) and (4.1), all terms on the right part of (4.2) are the known values. This allows computing the magnitudes $P_{n,m}^{k+1}$ in the left part of SLAE (4.2).

4. Conclusions

1. A method to predict flow in a straight rigid-walled duct with two rectangular axisymmetric narrowings has been developed. It has the second order of accuracy in the spatial and the first order of accuracy in the temporal coordinates, provides high stability of a solution, and requires much less computational time to obtain a result as compared to the methods available in scientific literature.

2. According to the method, the problem is solved by means of a) introducing the stream function and the vorticity with the corresponding transition from the Navier-Stokes and continuity equations, as well as the formulated initial and boundary conditions to appropriate relationships for the introduced variables; b) rewriting those relationships in a non-dimensional form; c) choosing appropriate computational domain and space-time computational mesh, and performing a corresponding discretization of the non-

dimensional relationships; d) solving the linear algebraic equations obtained after the use of the indicated discretization.

3. Performing the discretization, we apply the two-point temporal onward difference for the unsteady term, as well as the two-point backward differences (for the convective term of the non-linear vorticity equation) and the three-point approximations (for the diffusive term of the noted equation and Poisson's equations for the stream function and the pressure) in the axial and cross-flow coordinates. For discretization of the velocity components, the appropriate central differences are applied.

4. The linear algebraic equations for the stream function and the pressure (which are obtained after performing the discretization) are solved by the iterative successive over relaxation method. The obtained algebraic relationship for the vorticity is a complete computational scheme to determine this magnitude on the basis of the known values found at the previous instant of time.

REFERENCES

1. F. Azimpour, E. Caldwell, P. Tawfik, S. Duval, R.F. Wilson, "Audible coronary artery stenosis". *The American Journal of Medicine*, Vol. 125, pp. 515-521, 2016.
2. H.T. Banks, S. Hu, Z.R. Kenz, C. Kruse, S. Shaw, J. Whiteman, M.P. Brewin, S.E. Greenwald, M.J. Birch, "Model validation for a noninvasive arterial stenosis detection problem". *Mathematical Biosciences and Engineering*, Vol. 11, pp. 427-448, 2014.
3. J.H. Seo, R. Mittal, "A coupled flow-acoustic computational study of bruits from a modeled stenosed artery". *Medical and Biological Engineering and Computing*, Vol. 50, pp. 1025-1035, 2012.
4. S.S. Varghese, S.H. Frankel, "Numerical modeling of pulsatile turbulent flow in stenotic vessels". *Journal of Biomechanical Engineering*, Vol. 125, pp. 445-460, 2013.
5. M. Jahangiri, M. Saghafian, M.R. Sadeghi, „Numerical study of turbulent pulsatile blood flow through stenosed artery using fluid-solid interaction", *Computational and Mathematical Methods in Medicine*, Vol. 15, pp. 1-10, 2015.
6. R. Tabe, F. Ghalichi, S. Hossainpour, K. Ghasemzadeh, „Laminar-to-turbulence and relaminarization zones detection by simulation of low Reynolds number turbulent blood flow in large stenosed arteries", *Biomedical Materials and Engineering*, Vol. 27, pp. 119-129, 2016.
7. A.O. Borisyuk, "Experimental study of wall pressure fluctuations in rigid and elastic pipes behind an axisymmetric narrowing", *Journal of Fluids and Structures*, Vol. 26, pp. 658–674, 2010.
8. J. Garcia, O.R. Marrufo, A.O. Rodriguez, E. Larose, P. Pibarot, L. Kadem, "Cardiovascular magnetic resonance evaluation of aortic stenosis severity using single plane measurement of effective orifice area", *Journal of Cardiovascular Magnetic Resonance*, Vol. 12, pp. 1-12, 2012.
9. J. Garcia, M. Markl, S. Schnell, B. Allen, P. Entezari, P. Mahadevia, S.C. Malaisrie, P. Pibarot, J.Carr, A.J. Barker, "Evaluation of aortic stenosis severity using 4D flow jet shear layer detection for the measurement of valve effective orifice area", *Magnetic Resonance Imaging*, Vol. 32, pp. 891-898, 2014.
10. N. Srivastava, "Analysis of flow characteristics of the blood flowing through an inclined tapered porous artery with mild stenosis under the Influence of an inclined magnetic field", *Journal of Biophysics*, Vol. 14, pp. 1-9, 2014.
11. J.V. Reddy, D. Srikanth, "The polar fluid model for blood flow through a tapered artery with overlapping stenosis: effects of catheter and velocity slip", *Applied Bionics and Biomechanics*, Vol. 15, pp.1-12, 2015.
12. A. Zaman, N. Ali, O.A. Beg, "Numerical simulation of unsteady micropolar hemodynamics in a tapered catheterized artery with a combination of stenosis and aneurysm", *Medical and Biological Engineering and Computing*, Vol. 54, pp. 1423-1436, 2016.
13. N. Ali, A. Zaman, M. Sajid, J.J. Nieto, A. Torres, "Unsteady non-Newtonian blood flow through a tapered overlapping stenosed catheterized vessel", *Mathematical Biosciences*, Vol. 269, pp. 94-103, 2015.
14. A.O. Borysyuk, "A method to solve a problem of flow in a channel with two axisymmetric narrowings", *Science-Based Technologies*, Vol. 38, pp. 270-278, 2018. [in Ukrainian]
15. J. H. Ferziger, M. Peri´c, *Computational methods for fluid dynamics*, 3rd ed. Berlin: Springer, 2002. 424 p.

ЛІТЕРАТУРА

1. Azimpour F., Caldwell E., Tawfik P. Duval S., Wilson R.F. Audible coronary artery stenosis. *The American Journal of Medicine*, 2016. Vol. 125. P. 515-521.
2. Banks H.T., Hu S., Kenz Z.R., Kruse C., Shaw S., Whiteman J., Brewin M.P., Greenwald S.E., Birch M.J. Model validation for a noninvasive arterial stenosis detection problem. *Mathematical Biosciences and Engineering*. 2014. Vol. 11. P. 427-448.
3. Seo J.H., Mittal R. A coupled flow-acoustic computational study of bruits from a modeled stenosed artery. *Medical and Biological Engineering and Computing*. 2012. Vol. 50. P. 1025-1035.
4. Varghese S.S., Frankel S.H. Numerical modeling of pulsatile turbulent flow in stenotic vessels. *Journal of Biomechanical Engineering***.** 2013. Vol. 125**.** P. 445-460.
5. Jahangiri M., Saghafian M., Sadeghi M.R. Numerical study of turbulent pulsatile blood flow through stenosed artery using fluid-solid interaction. *Computational and Mathematical Methods in Medicine*. 2015. Vol. 15. P. 1-10.
6. Tabe R., Ghalichi F., Hossainpour S., Ghasemzadeh K. Laminar-to-turbulence and relaminarization zones detection by simulation of low Reynolds number turbulent blood flow in large stenosed arteries. *Biomedical Materials and Engineering*. 2016. Vol. 27. P. 119-129.
7. Borisyuk A.O. Experimental study of wall pressure fluctuations in rigid and elastic pipes behind an axisymmetric narrowing. *Journal of Fluids and Structures*. 2010. Vol. 26. P. 658–674.
8. Garcia J., Marrufo O.R., Rodriguez A.O., Larose E., Pibarot P., Kadem L. "Cardiovascular magnetic resonance evaluation of aortic stenosis severity using single plane measurement of effective orifice area. *Journal of Cardiovascular Magnetic Resonance*. 2012. Vol. 12. P. 1-12.
9. Garcia J., Markl M., Schnell S., Allen B., Entezari P., Mahadevia P., Malaisrie S.C., Pibarot P., Carr J., Barker A.J. Evaluation of aortic stenosis severity using 4D flow jet shear layer detection for the measurement of valve effective orifice area. *Magnetic Resonance Imaging*. 2014. Vol. 32. P. 891-898.
10. Srivastava N. Analysis of flow characteristics of the blood flowing through an inclined tapered porous artery with mild stenosis under the Influence of an inclined magnetic field. *Journal of Biophysics*. 2014. Vol. 14. P. 1-9.
11. Reddy J.V., Srikanth D. The polar fluid model for blood flow through a tapered artery with overlapping stenosis: effects of catheter and velocity slip. *Applied Bionics and Biomechanics*. 2015. Vol. 15. P.1-12.
12. Zaman A., Ali N., Beg O.A. Numerical simulation of unsteady micropolar hemodynamics in a tapered catheterized artery with a combination of stenosis and aneurysm. *Medical and Biological Engineering and Computing*. 2016. Vol. 54. P. 1423-1436.
13. Ali N., Zaman A., Sajid M., Nieto J.J., Torres A. Unsteady non-Newtonian blood flow through a tapered overlapping stenosed catheterized vessel. *Mathematical Biosciences*. 2015. Vol. 269. P. 94-103.
14. Борисюк А.О. Метод розв'язування задачі про течію в каналі з двома осесиметричними звуженнями. *Наукоємні Технології*. 2018. Том 38ю С. 270-278.
15. Ferziger J. H., Peri´c M. Computational methods for fluid dynamics, 3rd ed. Berlin: Springer, 2002. 424 p.

Borysyuk Andriy Oleksandrovych *– Doctor of Physical and Mathematical Sciences, Leading Research Fellow, Institute of Hydromechanics of the NAS of Ukraine, Zhelyabova Str., 8/4, 03680 Kyiv 180 MSP, Ukraine; e-mail: aobor@ukr.net; ORCID: 0000-0002-3878-3915.*

Борисюк Андрій Олександрович *- доктор фізико-математичних наук, провідний науковий співробітник, Інститут гідромеханіки НАН України, вул. Желябова, 8/4, 03680 Київ 180 МСП, Україна; e-mail: aobor@ukr.net; ORCID: 0000-0002-3878-3915.*

Борисюк Андрей Александрович *– доктор физико-математических наук, ведущий научный сотрудник, Институт гидромеханики НАН Украины, ул. Желябова, 8/4, 03680 Киев 180 МСП, Украина; e-mail: aobor@ukr.net; ORCID: 0000-0002-3878-3915.*

Надійшла – 10.12.2019.